NUMERICAL INVESTIGATION OF PREMATURE FATIGUE OF HIGH-SPEED TRAIN WHEELS IN PRESENCE OF FACETS DEFECT WITH CASE STUDY

Jouilel Naima[1]*, Mhaiti Nissrine[2], Radouani Mohammed[2], El Fahime Benaissa[2]

[1] *National School of Applied sciences, Abdelmalek Essaadi University, Tetouan, Morocco*
[2] *National High School of arts and crafts, Moulay Ismail University, Meknes, Morocco*
* naima.jouilel@gmail.com

In this paper, the premature failure of the high-speed railway wheel of power locomotive commissioned in Morocco since 2018 was investigated. A three-dimensional model of the wheel is established, with account of specific wheel's features, to perform the finite elements and modal analysis. Simulations were conducted for several functional diameters of wheels (850mm, 885mm, and 920mm) to figure out stress distribution in different operation conditions. Stress results show that the wheel bears the mechanical loading in both exceptional and fatigue loads, therefore a modal analysis of the structure in presence of facets, which create a vibratory state, is done to examine their effect on the premature fatigue of the wheel. Modal analysis reveals that the presence of facets leads to a vibratory mode near to resonance. Based on those results, critical operation points as function of facets number and wheel diameter were determined to avoid scenarios that lead to cracks and premature fatigue of the studied wheels. Existing maintenance procedures must be modified to overcome this problem and increase the wheel's lifetime without affecting the operation safety of the high-speed train.

Keywords: high speed railway locomotive wheel, facets, finite element analysis, modal analysis

1 INTRODUCTION

Morocco is the only African country to have a high-speed line (HSL) and continues to develop flagship projects to grow at a relatively rapid pace. The challenge of this project is central, as it is the first high-speed link within the African continent. The HSL is relatively transforming the rail network of a country whose traffic density was becoming worrying [1], [2]. The HSL is a rolling stock composed of 12 high-speed trains (HST) with very impressive characteristics allowing to reach a rolling speed of 350 Km/h. testing with this new rail network starts at the beginning of February, 2017. However, the first tests were carried out on shortened routes. Then, the last tests covered the entire length of the route, from Tangier to Marrakech [3] (Fig.1). The first HSL was commissioned on November 15th, 2018. Since the HST was commissioned, some defects have been detected at the level of locomotive wheels. These defects accelerate the periodicity of changing and generate extra charges. Thus, the morocco society of high-speed trains has launched a project whose objective is to detect the root causes of these cracks and premature failure of power locomotive wheels.

Prediction of fatigue cracking of industrial components under variable loads is still relatively rare due to the difficulties associated with calculating the stress intensity factor and the historical effects of loading[4]–[8]. These historical effects are largely due to the localized plastic deformation of the material at the crack tip. Among these, the delay effect after an overload is probably the most well-known. Moreover, the historical effects depend strongly on the cyclic elasto-plastic behavior of the material [9], [10]. As they result from the occurrence of residual stresses in the material in the vicinity of the crack end and in its wake [5]. To predict the rate of crack propagation taking into account the effects of localized plasticity, many authors have relied on local approaches to the problem using the finite element method [11], [12],[13].
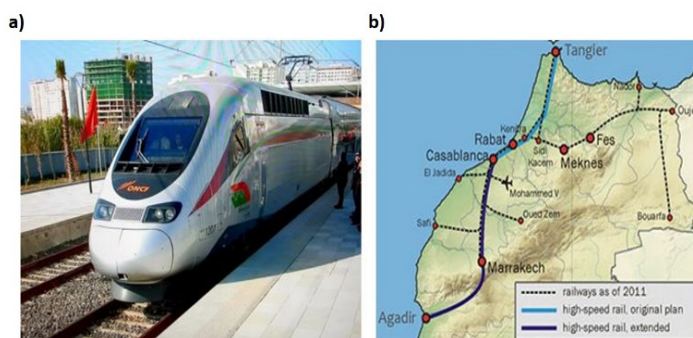

Figure 1. a) Moroccan High speed train b) Railway network

The high-speed trains are supported by multifunctional bogies ensuring passenger comfort and contact with the rail through the wheel which are exposed to damage in service and the phenomenon of fatigue [14]–[16]. The wheel-rail contact geometry relation is a basic problem in the rail transit systems. A mismatched wheel-rail surface will lead to serious problems for a running train, such as the instability and high contact stress between the wheel and rail, which

Journal of Applied Engineering Science

Vol. 21, No. 4, 2023

www.engineeringscience.rs

iipp publishing

Jouilel Naima et al. - Numerical investigation of premature fatigue of high-speed train wheels in presence of facets defect with case study

may further result in heavy tread wear, fatigue cracks, and high noise [17]–[20]. Wheels deformation appears according to different modes Until now there is no standard methodology for mixed mode testing, making it difficult to compare experimental results from different specimen geometries or testing apparatus. Wheel and rail materials were tested by Akama [21] using an in-plain biaxial testing machine. The fatigue crack growth behavior under mixed mode of a 60 kg rail steel, commonly used as a railroad track in Keren, was experimentally investigated by Kim and Kim, [20]The authors repainted that fatigue crack growth rate under mixed mode is slower than under model, and this difference decreases with the increase of the load R-curio. Tanaka, [22], presented a study on sheet specimens of aluminum in which the mixed mode is obtained by using an initial crack inclined so the tensile axis.

Wheel train defects in the rolling contact surface are classified into spalling facets and flat defects (Fig.2) [23][24], [25]. Herein, the effect of facets in generating a vibrational state is investigated. The objective is to figure out if there is a relation between premature fatigue and passing across a resonance state due to facets defects. Fig.3 resume the steps followed in this study.
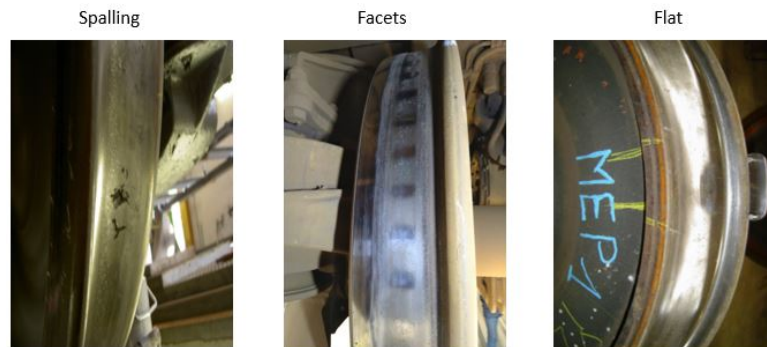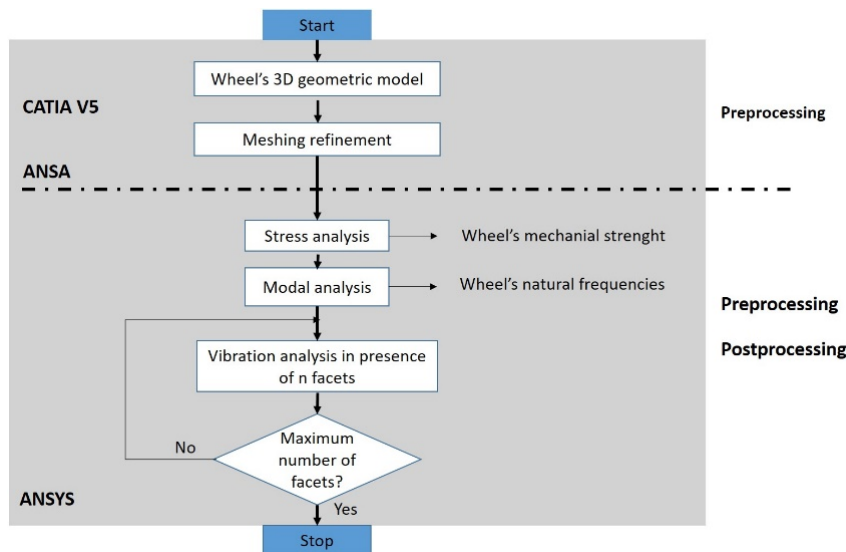

Figure 2. Types of wheel train defect

Figure 3. Block diagram of high-speed railway wheel's simulation steps

2 FINITE ELEMENT ANALYSIS FOR NUMERICAL MODELING

2.1 Geometric model and meshing criteria

This study concerns drive wheels with an exceptional geometry specific to high-speed trains as shown in fig.2. The railway language defines the different parts of wheels as follows:

- The running surface: this is the lateral surface of the rim; it ensures contact with the rail.
- The flange: a part of the wheel that guides the train when it passes through curves or on switches and crossings.
- The rim: a part of the heat-treated wheel that connects the wheel tread with the wheel plate.
- The wheel plate or web: it is the part limited by the hub and rim, it represents undulations whose purpose is to delay and dissipate the heat coming from contact with the rail so as not to reach the axis and the bearing boxes mounted at the ends of the axis.
- The hub: it is a larger part; it ensures the assembly by shrinking with the axis.

Elaborating wheel's geometric model is an important step. It consists in creating a numerical model that can describe and scan all the geometry, and as already mentioned, the geometry of high-speed wheels is specific. It contains dimensional features that must be treated with care such as the offset hole (a stress concentration zone, ensures the

Journal of Applied Engineering Science

Vol. 21, No. 4, 2023

www.engineeringscience.rs

iipp
publishing

Jouilel Naima et al. - Numerical investigation of premature fatigue of high-speed train wheels in presence of facets defect with case study

injection of high-pressure oil to offset the wheels from axles) and the wheel plate undulations. Fig. 5 (b) shows the cross-sectional view of the wheel with the offset hole.
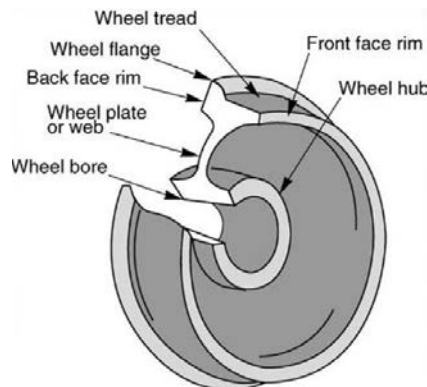

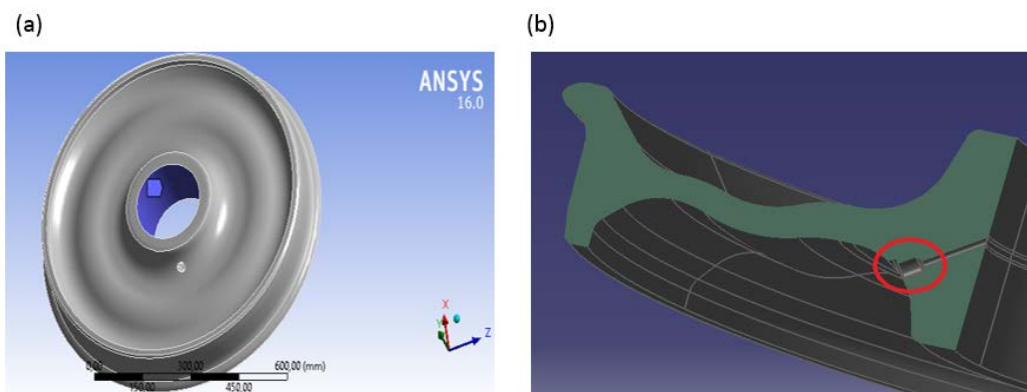Fig 4. Typical structure of high-speed railway wheel

Fig 5. (a) Wheel geometric model (b) Wheel section illustrating the offset hole and the undulations of the fabric

To conduct a Finite element analysis, hypothesis on wheel's material is taken. we remain in the isotropic linear elastic case and small deformations. That is to say:

- The wheels undergo small and reversible deformations.
- The law of behavior is linear.
- The wheel material behaves in the same way in all directions, Table 1 gives material properties.

Table 1 : Material properties (ER7)

Yield strength (MPa)	Tensile strength (MPa)	Young's modulus (MPa)	Poisson's ratio
450	710	210000	0,3

Model meshing is a step that conditions everything else in the calculation: the calculation time and resources (power of the machine), the results accuracy and convergence. Mesh configuration is an essential sub-step in finite element analysis: the finer the mesh, the less are gaps between simulation and reality, but the higher the cost of calculation would be. The importance of this step then requires special attention and proper treatment of the following points:

- Refinement in the areas of stress concentration.
- Refinement of the curves.
- Refinement at the load application points.
- Refinement in the sudden changes in the mechanical properties of the material.
- The size of the elements must be homogeneous throughout the structure.

To define an adequate 3D mesh, three types of meshes are distinguished. Meshing by tetrahedrons, hexahedrons, or prisms. Fig. 6 shows the three types. For a given mesh shape, the definition can focus on two main parameters: the size h, which is the radius of the sphere or circle in which it is written, and the degree p of the polynomial (Linear, quadratic or cubic). Thus, meshing refinement is either by decreasing h, or increasing p. In addition, for the same number of meshes a mesh with a high degree converges more [26], [27]. Therefore, to decide on the mesh size, let us remember that the wheels contain offset holes inducing a zone of stress concentration, and undulations in the wheel plate and are loaded punctually into the running surface. The one-piece wheel with a diameter of 850 mm, representing the wear limit which is the worst case, was meshed by triangular surface elements of one degree, then

Journal of Applied Engineering Science

Vol. 21, No. 4, 2023
www.engineeringscience.rs

iipp
publishing

Jouilel Naima et al. - Numerical investigation of premature fatigue of high-speed train wheels in presence of facets defect with case study

transformed into linear tetrahedrons to scan the volume of the structure. Fig (b) and Table 2 resumes meshing shape and details.
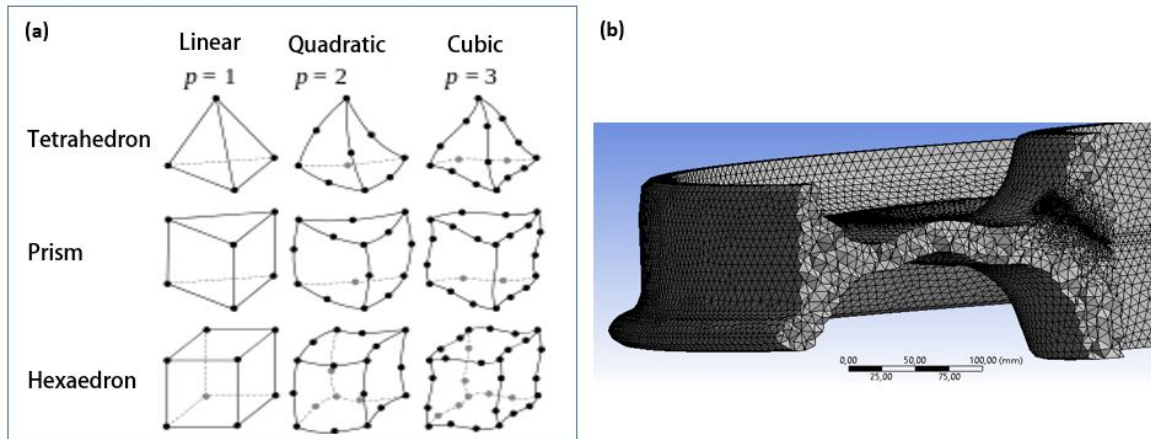

Fig*ure* 6. (a) Types of 3D meshes (b) Cross-sectional view of the section after refined mesh size

Table 2: mesh statistics for 850 mm wheel

Number of surface elements	72414
Number of volume elements	486580
Total number of nodes	723246

2.2   Loads modeling

Loads on wheels come from several sources acting at the same time or separately. The different stresses that affect the wheels are classified into two categories, exceptional and fatigue loads [28]. The different actions on wheels are as follows:

– The lift under the action of the vertical load of the power locomotive applied to the wheel-rail contact.
– The loading due to the transverse guidance that takes place at the flange-rail contact. It is not present or weak when the vehicle is in alignment and becomes important in curves.
– The switching during the passage of the train in the track changing devices causes a momentary reversal of the lateral force.

Fig.8 illustrates the loading for each case. The loads resulting from these stresses are difficult to calculate since they appear randomly with variable amplitudes. To model them, UIC leaflet 510 – 5 is used [29]. It is based on an AFNOR normative approach, specifically designed for the mechanical calculation of axles. Loads are defined as follows.

Exceptional loading: These forces are induced during the guidance in the curves.

Fatigue loads: UIC leaflet 510-5 defines the loads influencing wheel fatigue behavior as follows:

a) Loads on strut: These loads are induced during the passage of the curve.
b) Loads on needles: These forces occur when switching from one track to another.
c) Normal in-line load: This is the load in normal operation; no curve and no switch.

Values of loads used in simulation for each configuration are mentioned in fig. 8 and their application point in fig.9.
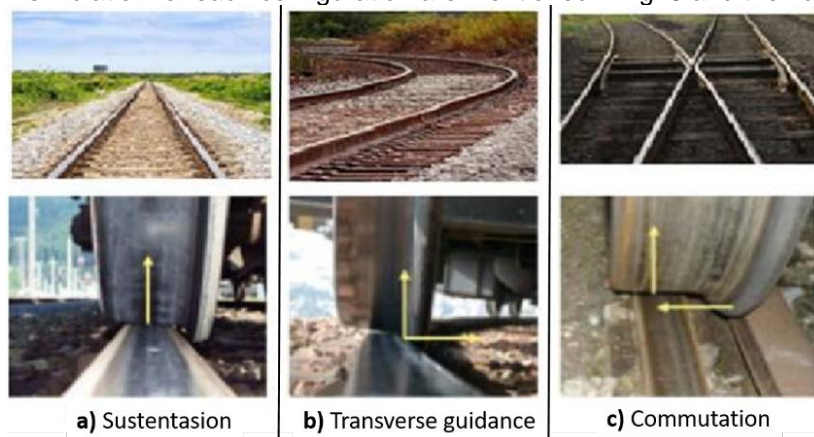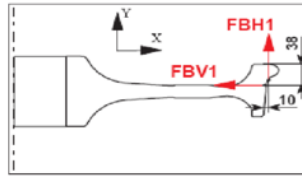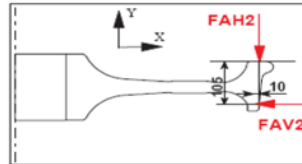

a) Sustentasion | b) Transverse guidance | c) Commutation

Figure 7. Loads applied in service

(a) Exceptional loading

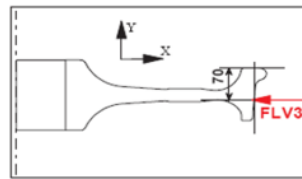| load	UIC 510-5
FBH1	67813 N
FBV1	160000 N

(b) Fatigue load

load	UIC 510-5
FAV2	108401 N
FAH2	36423 N

(c) Normal in-line load

load	UIC 510-5
FLV3	108401

Figure 8. Different load configuration according to UIC leaflet 510 – 5 [29]

1 Aligned traffic
2 Curved traffic
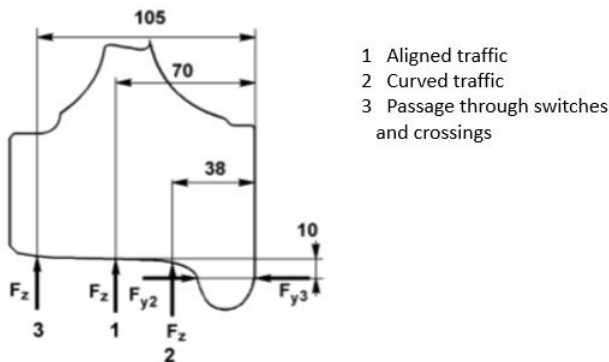3 Passage through switches and crossings

Figure 9. Load's application points

2.3   Wheel's model simulation results

Exceptional loads

In this part, the aim is to check the equivalent stresses of Von-Mises induced in the wheels at the limit state of wear during the passage of the trains in curvatures. Fig.10 shows the constraints mapping. Simulation results show that the constraints of Von-Mises are concentrated in the inner face of the canvases. Values in red are purely theoretical overloads in the part in contact with the rail.

It is concluded that the wheel remains always in the elastic zone since the stresses of Von-Mises in the web remain lower than the limit of elasticity (450 Mpa) given by NF EN 13 262 [30]. The maximum principal stress corresponds to the maximum constraint in traction. This is important when we wants to study the risks of cracks. Indeed, the use of a scalar equivalent stress such as the Von-Mises stress or the Tresca stress does not indicate whether a zone is subjected to strain, compression and / or shear. However, a constraint of the compression type is less dangerous because it tends to close the cracks in case of presence.

- Simulation results show that the main stresses are concentrated in the outer face of the web. This implies an area stressed in tension at the passage in curves.
- Parts of the offset hole which are also stressed in tension, but with acceptable stress values.
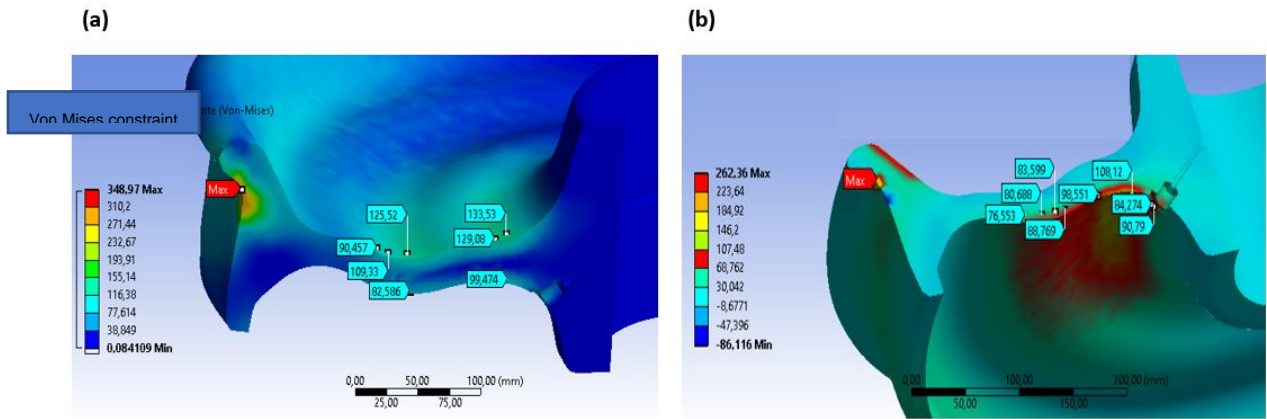
Journal of Applied Engineering Science

Vol. 21, No. 4, 2023
www.engineeringscience.rs

iipp
publishing

Jouilel Naima et al. - Numerical investigation of premature fatigue of high-speed train wheels in presence of facets defect with case study

(a) **(b)**

Figure 10. (a) Von-mises constraints for exceptional loading (b) Mapping of maximum stresses for exceptional loading

Fatigue loads

In this part, the aim is to check the fatigue resistance of the wheels by evaluating the alternating stresses. Therefore, each load case was treated separately, and the results were discussed case by case. Indeed, the technical homologation standard of monoblock wheels NF EN 13 979 proposes a study process to decide on wheel's validity according to fig.11 where $\Delta\sigma$ is the extent of the alternating stress and A is the permissible stress. The extent of the alternating dynamic stress in all points of the web must be less than the permissible fatigue stress which is 360 MPa. To determine the fatigue strength, the different loadings mentioned above were transformed into periodic functions. The fatigue behavior analysis yielded the following results:

– Coil loads: Concentration of alternating stresses in the inner face of the web with a maximum value of 62 MPa.
– Switching loads: concentration of alternating stresses in the outer face of the fabric with a maximum value of 48 MPa.
– Normal circulation load in line: concentration of alternating stresses in the outer face of the fabric with a maximum value of 24 MPa.

We deduce that the wheels are valid in fatigue without resorting to the second stage which is the passage to a bench testing since the extent of the dynamic alternating stress does not exceed the admissible limit.
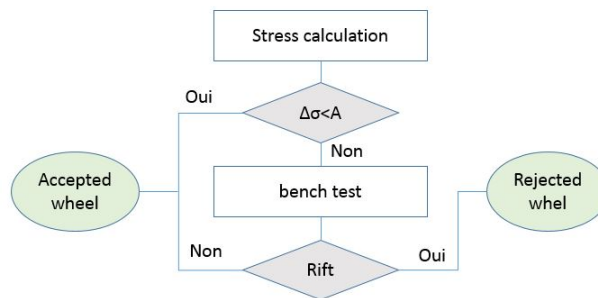
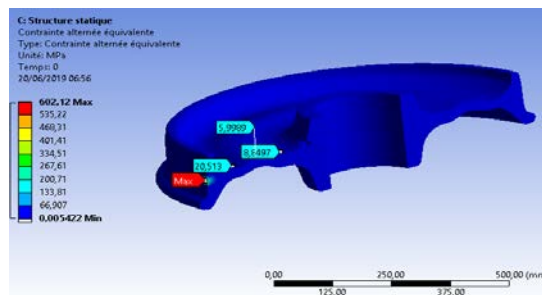Fig*ure* 11. Decision flowchart of wheel behavior in fatigue

Fig*ure* 12. Alternating stress / in-line traffic

3 MODAL ANALYSIS AND HARMONIC RESPONSE OF WHEELS

3.1 Mathematical formulas

High-speed wheels are exposed to external stresses that can lead to vibrations, therefore, modal analysis and harmonic wheel response like all mechanical structures, then an understanding of the dynamic behavior of the wheels

Journal of Applied Engineering Science

Vol. 21, No. 4, 2023

www.engineeringscience.rs

iipp
publishing

Jouilel Naima et al. - Numerical investigation of premature fatigue of high-speed train wheels in presence of facets defect with case study

is necessary in order to avoid and control the stresses that can lead to states of mechanical resonance. Indeed, any structure responds mainly to its resonance modes. Steel railway wheels have very low damping: their vibration behavior is marked by high-pitched resonances. Each resonance is characterized by a natural frequency, possibly complex to translate dissipative phenomena, and an associated deformation that forms a natural mode. The modes of a railway wheel are similar to those of a circular flat plate with a free edge.

The objective of this section is to give the different natural frequencies, then to treat the different possible cases of vibration. In system dynamics, any structure can be modeled by a set of masses linked together by springs and dampers in series, in parallel or in combination [31],[32]. For a good explanation, let's take the case of a simple non-damped system modelled by two masses and three springs. Considering two mass-spring systems, of the same masses m1=m2=m. These are each connected to a rigid support by springs of the same stiffness noted k, and coupled by another stiffness spring K. The non-damped assembly can move horizontally with negligible friction (fig.13).
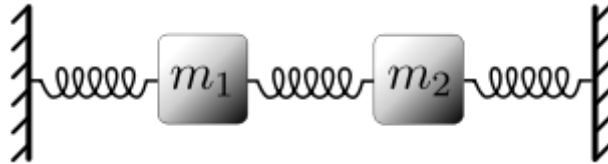

Fig*ure* 13. System with 2 degrees of freedom modelled by two masses and three springs

The equations of motion are:

$$\begin{pmatrix} m\ddot{x}_1(t) \\ m\ddot{x}_2(t) \end{pmatrix} = \begin{bmatrix} -(K+k) & K \\ K & -(K+k) \end{bmatrix} \begin{pmatrix} x_1(t) \\ x_2(t) \end{pmatrix} \tag{1}$$

The next step is then to search for harmonic solutions of pulsation ω to this matrix with differential equation, by posing $\overrightarrow{x_\omega} = \overrightarrow{x_m}.e^{jwt}$

It is obvious that $\overrightarrow{\ddot{x_\omega}} = -\omega^2.\overrightarrow{x_\omega}$ and the matrix equation is then reduced to an eigenvalue equation (2).

$$[K].\overrightarrow{x_\omega} = -m.\omega^2.\overrightarrow{x_\omega} \tag{2}$$

$$Det([K]+m\omega^2.[I])=0 \tag{3}$$

Then ω is the solution of equation 3, with [K] the stiffness matrix and $.[I]$ matrix of inertia 2x2.

This method has the advantage of being generalizable, at least in theory, to any number of degrees of freedom and to more general situations, with different masses or stiffnesses, but it can also result in rather heavy calculations, hence the need for numerical calculation methods. For the three-wheel diameters: 920 mm, 885 mm, 850 mm, the natural frequencies and their deformation modes were derived with finite element modal analysis. The wheels of high-speed trains running at a speed of 320 km/h have a high rotation frequency that depends on the diameter. Excitation frequencies are as follows. We have to notice that the excitation frequency is calculated by multiplying the number of facets by the rotation frequency.

- 920 mm wheel: rotation frequency 30.75 Hz
- Wheel 885 mm: rotation frequency 31.97 Hz
- Wheel 850 mm: rotation frequency 33.33 Hz

Facets appearing in the treadmill are often located in the center of the treadmill and coincide with the point of application of the normal in-line traffic force FLV3. This leads to a state of cyclical excitation by this force. Frequency response of the wheel subjected to FLV3 force can be determined from its vibration modes. Let us introduce this by considering a damped system with a degree of freedom of mass type M, spring K, damping C. The complex amplitude u of the mass displacement is given by the equation of motion:

$$-\omega2Mu+i\omega Cu+Ku=FLV3 \tag{4}$$

The expression of the own pulse ωi and the damping factor ζi are given by:

$$\omega i =\sqrt{K/M} \tag{5}$$

$$\zeta i = C\ 2\ \sqrt{KM} \tag{6}$$

Allow to write the expression (4) in the form:

$$M(\omega_i^2 -\omega^2 + 2i\zeta_i\omega\omega_i)u = FLV3 \tag{7}$$

Thus, the mobility, which is the ratio between the vibratory velocity and the force applied at the same point, and which represents the ability of a structure to vibrate for a unitary force, is given by:

Journal of Applied Engineering Science

Vol. 21, No. 4, 2023

www.engineeringscience.rs

iipp
publishing

Jouilel Naima et al. - Numerical investigation of premature fatigue of high-speed train wheels in presence of facets defect with case study

$$Y = \frac{iu\omega}{FLV3} = \frac{i\omega}{M(\omega_i^2 - \omega^2 + 2i\zeta_i\omega\omega_i)} \tag{8}$$

More generally, when the first N Eigen modes Φ_n are known, the response of a structure at point j for a pulsation force ω (f=2π) applied ink is obtained by modal superposition:

$$Y_{jk} = \sum_{i=1}^{N} \frac{i\omega\Phi_{ji}\Phi_{ki}}{m_i(\omega_i^2 - \omega^2 + 2\zeta_i\omega\omega_i)} \tag{9}$$

Where Φ_{ji} is the amplitude of mode i at position j, Φ_{ki} is the amplitude of mode i at position k, and mi is the generalized mass. The pulsation ω_i, the amplitude Φ_i and the generalized mass mi of each mode i are calculated by the finite element method.

3.2   Deformation modes

A natural mode is a spatial form in which an excitable system (micro or macroscopic) can oscillate after having been disturbed near its stable equilibrium state, a natural frequency of vibration is then associated with this form. The natural frequency is the frequency with which this system oscillates when it is in free evolution, that is to say without external excitatory force nor dissipative forces (friction or resistance for example). This notion is fundamental to understand the phenomena of excitation, and resonance. A natural mode or normal mode, is a spatial form according to When a system is excited cyclically, it could resonate with one of the eigen frequencies associated with the different eigen modes. It is a consideration that should never be missed during the mechanical or civil verification, for example, it is important to determine the natural frequencies of a structure to ensure that in the conditions of use, the external excitations do not coincide not with the clean modes[33], [34].

- Radial mode Rn: The most important deformations during the vibrations are carried by a radial axis (nodal diameter). The number n means the number of its radial axes.
- Model mLn: the most important deformations are not carried by the nodal diameters. m is the number of section planes containing nodal circles. n is the number of nodal diameters.
- The 0 nodal circle mode induces lateral bending of the section.
- The radial mode corresponds to the tension / compression of the fabric in the radial direction.
- The 1-nodal circle mode. The wheel section has a second lateral bending movement. The tilting movement of the bandage is important.
- The 2 nodal circle mode, the deformation of the cross section corresponds to a third mode of lateral bending with a first nodal circle in the center of the fabric and a second at the base of the bandage.
- The nodal circle is a circle illustrating an area which undergoes a displacement but no deformation during the vibrations, analogically plays the role of the neutral fiber in the case of the bending or torsion of a beam. The following figure shows the mode 1L1 of the 920mm wheel with a location of nodal circles in the rims.
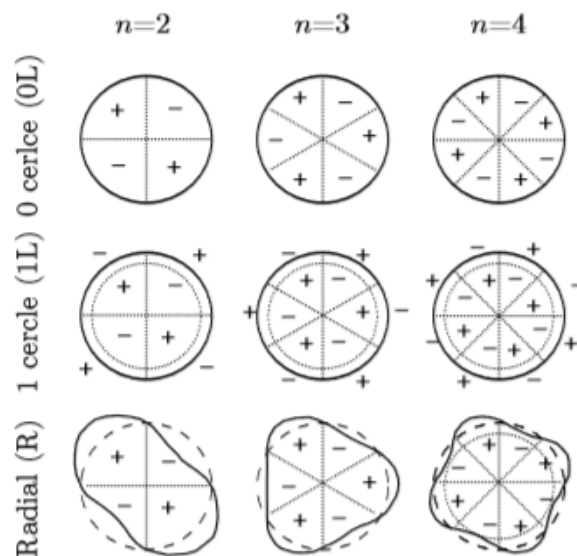

Figure 14. Examples of wheel's modal deformities, Signs +/- indicate the relative phase of the deformations, (- - -) undistorted state, (---) deformed state and (···) nodal lines
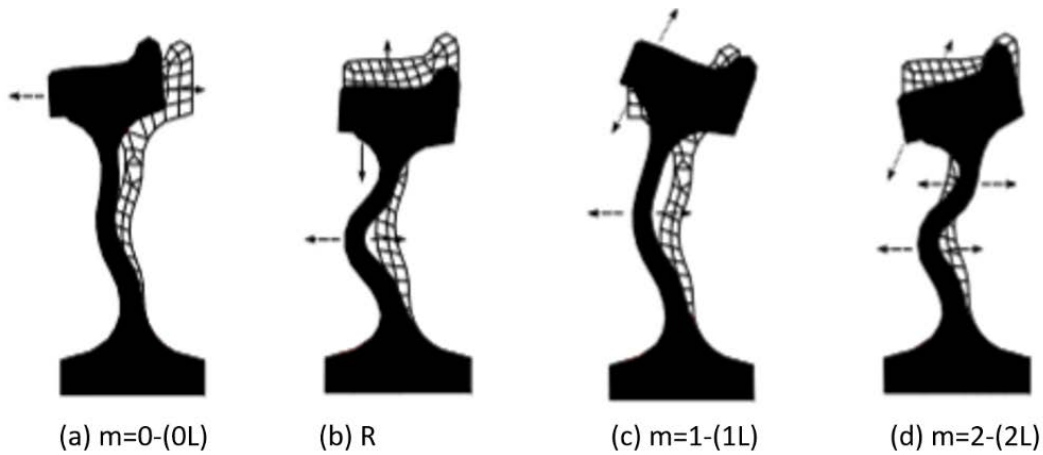
Journal of Applied Engineering Science

Vol. 21, No. 4, 2023

www.engineeringscience.rs

iipp
publishing

Jouilel Naima et al. - Numerical investigation of premature fatigue of high-speed train wheels in presence of facets defect with case study

(a) m=0-(0L)   (b) R   (c) m=1-(1L)   (d) m=2-(2L)

Fig*ure* 15. Modal deformations of the cross section of a one-piece wheel; lateral (- ->), vertical (→) and coupled (--->) movements
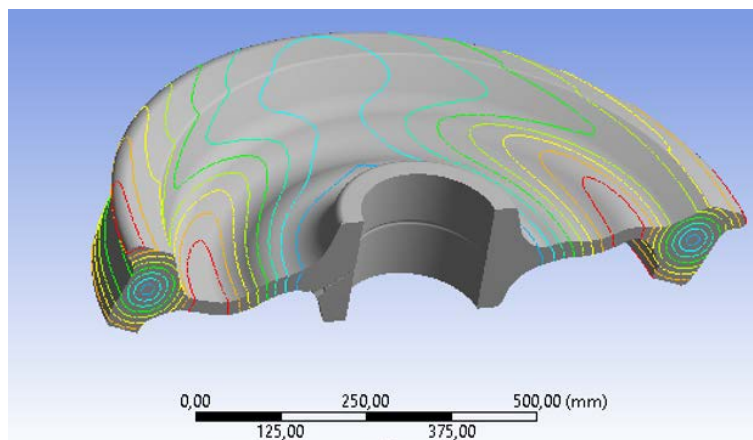

Figure 16. Mode 1L1 / 920 wheel

3.3 Results

The law of appearance of facets is not yet mastered; therefore, a case study is needed to verify the different possible configurations. The harmonic response of the HST wheels has been calculated by ANSYS and modal superposition method is adopted in a frequency range from 0 to 2500 Hz. Table 3 gives the mesh statistics for each wheel. Fig.17 shows the harmonic responses of the 920mm, 885mm and 850mm wheels for cyclic excitation FLV3 in the section containing the offset hole.

Firstly, and for 920 mm wheel, we notice a high peak around 1800 Hz leading to R2 mode with a maximum equivalent stress of 116.49 MPa. Secondly, a peak around 1950 Hz leading to R2 mode with a maximum equivalent stress of 56,713 MPa is noticed for 885 mm wheel. Concerning the peak in the 2437 Hz frequency, the existent wheels do not reach such high frequencies. Finally, for 850mm wheel, we notice a high peak around 1540 Hz leading to RI mode, and another peak around 2000 Hz leading to 2L2 mode but with a low stress value of 35 Mpa.
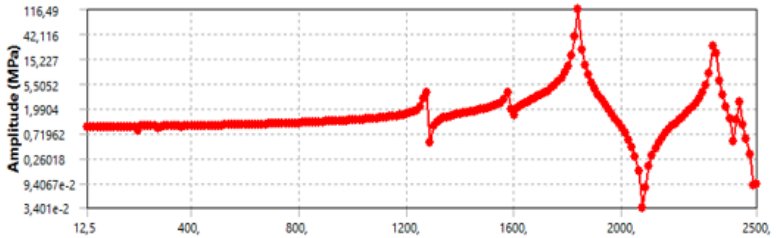
Table 3: Mesh statistics for each wheel diameter

Diameter (mm)	920	885	850
Number of elements	934348	919983	920948
Number of knots	1417709	1395919	1393778

(a) harmonic response of 920 mm wheel
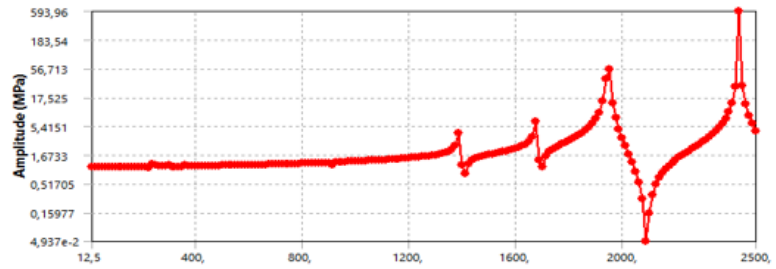
(b) harmonic response of 885 mm wheel
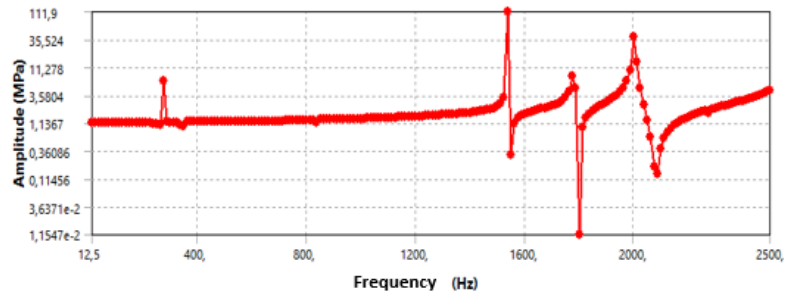
(c) harmonic response of 850 mm wheel

Figure 17. Wheels harmonic responses

Modal analysis made it possible to extract the different natural frequencies for different diameters of the morocco high-speed wheels. Then the case study synthesized by the previous tables made it possible to understand the dynamic behavior with a speed of 320 km/h of the wheels following the excitations generated by facets defects. We can conclude that well-defined numbers of facets lead the wheels to a vibratory state of resonance or near resonance. Summarize the study's results, Table 4 gives each wheel's mode of deformation according to a specific number of facets. All the critical Eigen modes found affect the wheel cover, except for the OL4/920mm mode which mainly affects the flange Therefore, to avoid resonance states, the following critical operation points must be eliminated: (920 mm, 56, 320 km/h); (920 mm, 60, 320 km/h); (885 mm, 60, 320 km/h); (885 mm, 61, 320 km/h); (850 mm, 60, 320 km/h): (850 mm, 62, 320 km/h). Either by wheels re-profiling before reaching critical numbers of facets or by decreasing and increasing wheel rotation frequency to maintain the same travel time.

Table 4: Number of facets and their deformation modes for 920mm, 885mm and 850 mm diameter of wheels

Wheel's diameter (mm)	Facets	Deformation mode
920	56	0L4
	60	R2
885	60	1L1
	61	R2
850	60	2L2
	62	1L1

To guarantee functional adherence, and therefore optimal safety, each wheel must have a perfectly round and symmetrical shape. Under the operating conditions, the wheels of the RGVM are damaged and the wheels lose their original shape. Each axle of each train set is therefore subject to very precise monitoring and constant readings to correct dimensional deviations in the wheel tread. Re-profiling is then essential and makes it possible to correct the facets and irregularities of the wheels, it is a question of machining the wheels, to restore a perfect running surface. For this purpose, the morocco high speed train maintenance company position the trains on what is called "a pit lathe", which is a numerically controlled machine. This installation makes it possible to carry out certain necessary maintenance operations under the trainset, without dismantling or changing their composition, which represents a significant time saving.

Journal of Applied Engineering Science

Vol. 21, No. 4, 2023

www.engineeringscience.rs

iipp
publishing

Jouilel Naima et al. - Numerical investigation of premature fatigue of high-speed train wheels in presence of facets defect with case study

Figure 18. Wheel inspection operation

4 CONCLUSION

The objective of this study is to investigate the premature failure of HST wheels in Morocco. Firstly, a mechanical behavior modeling is done. It allows the establishment of tridimensional wheel model and then a finite element analysis is conducted. By combining exceptional and fatigue loads, FEM results show that wheels bear the mechanical loading. Secondly, a modal analysis is carried to figure out natural frequencies of the system and their deformation modes, in order to visualize the areas most affected by each natural mode in case of resonance or close to resonance.

Railway wheels, with their special geometrical characteristics and special composition (material), have acute resonance states and are exposed to vibrations during operation caused by wear defects such as facets. The case study of the existence of facets in the wheel tread made it possible to synthesize the vibration behavior for different wheel diameters (920mm, 885mm, and 850mm). Critical operation points were enumerated and must be avoided to protect the structure from resonance phenomena and from the risk of cracks and derailment. Wheel's re- profiling is proposed as a solution against facets defects, even if it is not required in the maintenance documents.

5 ACKNOLEDGEMENT

6 REFERENCES

[1] M. R. Khlie, R. M. Vi, W. Economic, and L. G. V. C.- Tanger, "Les LGV , un levier principal pour le développement de la mobilité, des territoires et du tissu é conomique (DG de l ' ONCF)," vol. 2016, 2018.

[2] M. C. Cambon, "Le Maroc à l'Heure du TGV," 2012.

[3] "https://www.morocco-guide.com/transport/train-in-morocco/." .

[4] Y. Lu, P. Xiang, P. Dong, X. Zhang, and J. Zeng, "Analysis of the effects of vibration modes on fatigue damage in high-speed train bogie frames," Eng. Fail. Anal., vol. 89, no. November 2016, pp. 222–241, 2018, doi: 10.1016/j.engfailanal.2018.02.025.

[5] A. Naderi, "Numerical investigation on stress intensity factor in railway wheel-set under the influence of residual stresses induced by press fitting process," Eng. Fail. Anal., vol. 94, no. March, pp. 78–86, 2018, doi: 10.1016/j.engfailanal.2018.07.029.

[6] D. F. C. Peixoto and P. M. S. T. de Castro, "Fatigue crack growth of a railway wheel," Eng. Fail. Anal., vol. 82, no. July, pp. 420–434, 2017, doi: 10.1016/j.engfailanal.2017.07.036.

[7] Y. Z. Chen, C. G. He, X. J. Zhao, L. B. Shi, Q. Y. Liu, and W. J. Wang, "The influence of wheel flats formed from different braking conditions on rolling contact fatigue of railway wheel," Eng. Fail. Anal., vol. 93, no. July, pp. 183–199, 2018, doi: 10.1016/j.engfailanal.2018.07.006.

[8] C. Zhu, J. He, J. Peng, Y. Ren, X. Lin, and M. Zhu, "Failure mechanism analysis on railway wheel shaft of power locomotive," Eng. Fail. Anal., vol. 104, no. March, pp. 25–38, 2019, doi: 10.1016/j.engfailanal.2019.05.013.

[9] B. Gao et al., "Influence of non-uniform microstructure on rolling contact fatigue behavior of high-speed wheel steels," Eng. Fail. Anal., vol. 100, no. March, pp. 485–491, 2019, doi: 10.1016/j.engfailanal.2019.03.002.

[10] L. GENTOT, S. POMMIER, W. D'HARDIVILLIERS, and F. COCHETEUX, "Prévision de la fissuration par fatigue de roues de train portant des disques de frein flasqués," in 19 ème Congrés Franç̧ais de Mécanique, 2009, pp. 1–6.

[11] M. Gzaiel, E. Triki, and A. Barkaoui, "Finite element modeling of the puncture-cutting response of soft material by a pointed blade," Mech. Mater., vol. 136, 2019, doi: 10.1016/j.mechmat.2019.103082.

[12] K. J. Bathe, "The AMORE paradigm for finite element analysis," Adv. Eng. Softw., vol. 130, no. October 2018, pp. 1–13, 2019, doi: 10.1016/j.advengsoft.2018.11.010.

[13] Y. Lee, N. Ogihara, and T. Lee, "Assessment of finite element models for prediction of osteoporotic fracture," J. Mech. Behav. Biomed. Mater., vol. 97, no. December 2018, pp. 312–320, 2019, doi: 10.1016/j.jmbbm.2019.05.018.

[14] K. R. Kashyzadeh and G. H. Farrahi, "Improvement of HCF life of automotive safety components considering a novel design of wheel alignment based on a Hybrid multibody dynamic, finite element, and data mining techniques," Eng. Fail. Anal., vol. 143, no. 1, pp. 88–100, 2022.

[15] H. Zhang, X. Yang, C. Xie, G. Tao, H. Wang, and Z. Wen, "Experimental investigation of effect of wheel out-of-roundness on fracture of coil springs in metro vehicles," Eng. Fail. Anal., vol. 142, 2022, doi: 10.1016/j.engfailanal.2022.106811.

[16] C. Liu, J. Xu, K. Wang, T. Liao, and P. Wang, "Numerical investigation on wheel-rail impact contact solutions excited by rail spalling failure," Eng. Fail. Anal., vol. 135, 2022, doi: 10.1016/j.engfailanal.2022.106116.

[17] L. Wang, P. Wang, S. Quan, and R. Chen, "Contact Geometry Relationship in a Turnout Zone," J. Mod. Transp., vol. 20, no. 3, pp. 148–152, 2012, doi: 10.1007/BF03325792.

[18] X. Jiang, X. Li, X. Li, and S. Cao, "Rail fatigue crack propagation in high-speed wheel/rail rolling contact," J. Mod. Transp., vol. 25, no. 3, pp. 178–184, 2017, doi: 10.1007/s40534-017-0138-6.

[19] C. Yang, F. Li, Y. Huang, K. Wang, and B. He, "Comparative study on wheel-rail dynamic interactions of side-frame cross-bracing bogie and sub-frame radial bogie," J. Mod. Transp., vol. 21, no. 1, pp. 1–8, 2013, doi: 10.1007/s40534-013-0001-3.

[20] J. K. Kim and C. S. Kim, "Fatique crack growth behavior of rail steel under mode I and mixed mode loadings," Mater. Sci. Eng. A, vol. 338, no. 1–2, pp. 191–201, 2002, doi: 10.1016/S0921-5093(02)00052-7.

[21] M. Akama, "Fatigue crack growth under mixed loading of tensile and in-plane shear modes," 2003. doi: 10.1111/j.1944-9720.2000.tb01995.x.

[22] K. Tanaka, "Fatigue crack propagation from a crack inclined to the cyclic tensile axis," Eng. Fract. Mech., vol. 6, no. 3, pp. 493–507, 1974.

[23] L. Han, L. Jing, and K. Liu, "A dynamic simulation of the wheel–rail impact caused by a wheel flat using a 3-D rolling contact model," J. Mod. Transp., vol. 25, no. 2, pp. 124–131, 2017, doi: 10.1007/s40534-017-0131-0.

[24] T. Roy, "Elimination of surface defects in high tensile steel for wheel rim applications," Eng. Fail. Anal., vol. 17, no. 1, pp. 93–99, 2017.

[25] T.Nowakowski, P. Komorski, and G. M. S. and F. Tomaszewski, "Wheel-flat detection on trams using envelope with Hilbert transform," Solids Struct., vol. 16, no. 5, pp. 1–16, 2019.

[26] F. Rieg, R. Hackenschmidt, and B. Alber-Laukant, Finite Element Analysis for Engineers. HANSER, 2014.

[27] Q. Y. Xiong, S. T. Yu, and J. S. Ju, "Fatigue analysis on wheel considering contact effect using FEM method," Math. Probl. Eng., vol. 2015, 2015, doi: 10.1155/2015/314634.

[28] SKF-Group, Railway technical handbook, vol. 2, no. 2. 2012.

[29] "Technical approval of monobloc wheels - application document for standard en 13979- 1," p. 13979.

[30] AFNOR, "NF DTU 13.2-1-1 Indice," 2018.

[31] D. A. Crolla, Automotive Engineering Powertrain, Chassis System and Vehicle Body. Elsevier, 2009.

[32] N. Lobontiu, System dynamics for Engineeringstudents. Elsevier, 2010.

[33] G. S. Guoyan Zheng, Shuo Li, Statistical Shape and Deformation Analysis. 2017.

[34] B. Yang, Stress, Strain, and Structural Dynamics. 2005.